A DETERMINISTIC MODEL FOR SNOWDRIFT ACCUMULATION[1]

Neil H. Berg[2]

Abstract.--A set of hypotheses concerning the development of snowdrifts on natural alpine terrain was transformed into a model predicting the location and extent of snowdrift accumulation. Windspeed and snowfall rate are the primary dynamic inputs to the model. Field measurements at two sites on Niwot Ridge in the Colorado Front Range were used to analyze the model. It appears to be sensitive to changes in the threshold windspeed for the initiation of grain deposition and the delimitation of the lower boundary of the atmospheric mixing region. Windspeed is the dominant determinant for accumulation rate; maximum accumulation rates occur at moderate windspeeds. The model must be validated before it can be used in an operational setting.

INTRODUCTION

In geographic regions of seasonal snow accumulation where woody vegetation is scarce, redistribution of fallen snow by wind is common. Lee-slope depressions in the ground topography play an important role by acting as catchments for blowing snow. The result of the redistribution process is striking in late spring and early summer when snow may remain only adjacent to drainage channels in high plains regions or to the lee of alpine solifluction terraces.

Understanding of the relationships between topography and snow redistribution is incomplete, and much is qualitative. Natural snowdrift formation relates to loading in avalanche catchments and hence avalanche magnitude and frequency (Perla and Martinelli 1976). Drift formation is a central factor in maintaining "drift" or Ural-type glaciers (Outcalt and MacPhail 1965), and drift accumulations can augment late season water supplies (Martinelli 1975). Drifts can also influence microscale treeline distribution (Minnich 1984). This paper examines the role of wind-driven snow in the mass budget of alpine snowbanks. It also describes the development of and experimentation with a quantitative model for snowdrift accumulation.

A set of hypotheses was developed addressing why snowdrifts accumulate at some topographic locations. These hypotheses formed a conceptual model of drift development based upon the physical processes that result in snow transport and deposition. The conceptual model was then transformed into a mathematical model. With reasonable assumptions about most of the input values, precipitation rate, windspeed, and ground topography information become the only variables requiring observed data. The mathematical model was tested by comparison with empirical data. Two compatible data sets were developed: one incorporated model outputs, the other used field observations of drift accumulations in nature. The empirical observations were limited to two drifts observed for 2 years. More data and testing are needed before statistical validation of the model is complete. The model cannot now be used for operational decisions.

MODEL DEVELOPMENT

The primary aim of the model is to determine deposition locations for wind-blown snow particles. Deposition occurs when the tractive force of the air flow is no longer sufficient to transport the particles. Such a reduction in force, as produced by a decrease in windspeed, can be caused by changes in topography. If the flow boundaries narrow, wind shear increases, and particles may be eroded from the snow surface. Conversely, expanding flow--downslope or into topographic depressions--decreases windspeed and wind shear and promotes particle deposition. The model comprises a set of mathematical relationships among airflow, ground topography, and particle movement that determine locations where the windspeed is below the threshold needed for snow particle transport.

Ground topography is the primary static input to the model. Windspeed and wind direction over varied terrain define the tractive force for

---

[1]Paper presented at the International Snow Science Workshop, Lake Tahoe, California, October 22-25, 1986.

[2]Neil H. Berg is Supervisory Hydrologist, Pacific Southwest Forest and Range Experiment Station, Forest Service, U.S. Department of Agriculture, Berkeley, Calif.

particle movement. From knowledge of the ground topography and airflow across it, locations may be identified as potential drift accumulation sites. The model quantifies particle transport and specifies trajectories with respect to the ground and airflow parameters. A final component of the model specifies the depositional mechanisms controlling particle settlement.

Ground Topography

A two-dimensional Cartesian coordinate system is used to specify changes in distance and height from a reference point. Input topographic data consist of up to 50 x-z coordinate pairs specifying the terrain breaks. In its simplest form, a terrain break resembles a step (fig. 1).

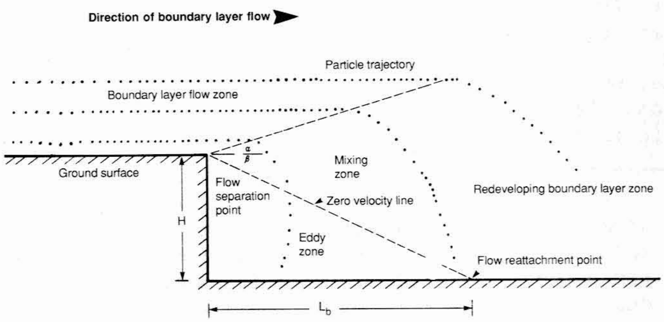

Figure 1.--Schematic representation of airflow streamlines, particle trajectories, and airflow zones across a topographic step.

Airflow Speed

In the airflow component of the model, the ultimate objective is estimation of horizontal and vertical windspeeds at and near steps. Extensive theoretical and empirical analyses of airflow across steps have been made. Four zones of airflow are important (fig. 1): (1) upwind of a step in a zone of undisturbed boundary layer flow; immediately downwind of a step in (2) mixing and (3) eddy zones; and (4) beyond a step in a region of redeveloping boundary layer flow.

Upwind of a step, flow speed is assumed to increase logarithmically with height (Schmidt 1972, Budd et al. 1966)

$$U_* = U_z K [\ln (z/z_o)]^{-1} \text{ where} \tag{1}$$

U_* is the frictional flow speed (m s^{-1}),
U_z is horizontal windspeed (m s^{-1}) at height z (m),
K is the von Karmen coefficient, and
z_o is the roughness element (m).

When the flow crosses the crest of a slope and enters a topographic depression (the lee of a step) flow streamlines diverge, speed decreases, and an eddy zone of reversed flow develops. This zone is bounded by the ground surface below and a line (in the two-dimensional case) of zero velocity above (fig. 1). The zero velocity line intersects the ground surface downstream at the point of flow reattachment. Boundary layer flow separates at sharp step or terrain discontinuities. Above the line of zero velocity, a mixing zone develops that is characterized by increasing turbulence and growing vortices.

Flow calculations for the eddy and mixing zones are based upon theoretical considerations and empirical measurements of flow in full and half jets (Abramovich 1963, Naib 1966). In the mixing and eddy zones horizontal flow speeds are calculated as

$$U_{z,x} = U_{m,x}-(1-N^{1.5})^2 (U_{m,x}-U_{b,x}) \tag{2}$$

where $N = (z-z_{b,x}) (z_{m,x}-z_{b,x})^{-1}$,

$U_{z,x}$ is flow speed at height z and horizontal distance x from the separation point,
$U_{m,x}$ is the maximum forward flow speed at the upper boundary of the mixing zone at x,
$U_{b,x}$ is the maximum reverse flow speed in the eddy zone at x, and
$z_{b,x}$ and $z_{m,x}$ are the heights at which $U_{b,x}$ and $U_{m,x}$ occur (Naib 1966).

The spatial configuration of the mixing and eddy zones is controlled largely by the upper (α) and lower (β) angles in the mixing zone (fig. 1). Water flume and wind tunnel experimentation, and theoretical analyses give values of α ranging from 5^o to 6.1^o (Jopling 1960, Naib 1966). The mean of these values, 5.4^o, is used by the model unless the user specifies otherwise. Determination of β follows from the relationship between step height, H, and separation bubble length, L_b (fig. 1). Data on flow in reattaching jets and half-jets (Allen 1968:157) relate L_b/H via the boundary layer thickness, h. Given H and h, L_b can be calculated and β becomes the arctangent of H/L_b.

Beyond the point of flow reattachment the fourth flow zone is characterized by redevelopment of a boundary layer flow similar to that upwind of the separation point. In this zone, flow characteristics gradually revert to those which follow the logarithmic profile law. More specific mathematical representations of the airflow in the four zones, and of other components of the model are described elsewhere (Berg 1977).

Particle Load

At low temperatures, blowing snow particles may be considered to be hard ice spheres approximately 0.1 mm in diameter (Mellor 1965). In many respects these spheres move like sand grains. Distinctions between snow and sand, however, are the inherent thermodynamic instability of snow particles, and the consequent importance of the sublimation of wind-blown snow and the cohesion of deposited snow particles.

One component of the model quantifies snow particle mass moving through the four airflow zones. First, total mass transport is apportioned among three modes of particle movement--saltation, creep, and suspension--in the zone of undisturbed boundary layer flow upwind of a step. The terminal velocity of fall, w, for particles of diameter, D, is calculated as

$$w = cD \text{ (D in mm, w in m s}^{-1}\text{)} \tag{3}$$

where c equals $2.2 \times 10^3 \text{ s}^{-1}$ for angular particles, 2.7 for subangular to subrounded particles, and 3.2 for round blowing snow particles (Budd 1966:60, Mellor 1965:12). Use of equation (3) assumes uniform, spherical particles that do not change size with height. At continental sites where significant drift occurs during otherwise quiescent, interstorm periods (Berg 1986), the sphericity assumption is not unrealistic (Schmidt 1972). But the assumption of particle size uniformity with height is incorrect, and equation (3) must be modified to calculate a nondimensional fall velocity, w_*, as

$$w_* = w\,(K\,U_*)^{-1} \tag{4}$$

where K and U_* are as defined above.

Given a snow transport quantity, q (g $\text{cm}^{-1}\ \text{s}^{-1}$), of particles of diameter d (cm), the fraction of q transported by suspension becomes P(W) (after Radok 1968), the remainder of q allocated to creep and saltation:

$$P(W) = (2/\pi)^{0.5} \int_{0.36w_*}^{\infty} e^{-x/2}\,dx \tag{5}$$

The suspension load, q_{sus}, equals q P(W). To facilitate computation of the suspension load, the lower atmospheric boundary layer is segmented into layers. The "drift density" or suspended snow particle mass (g m^{-3}), n_z, at height z can be calculated from the following relationship (Mellor and Radok 1960)

$$n_z = n_{z(1)}\,[z/z(1)]^{-w*} \tag{6}$$

where $n_{z(1)}$ is the drift density at z(1). By rearranging equation (6) so that the ratio $n_z/n_{z(1)}$ becomes the argument and considering z(1) as the height of the lowest suspension load layer, suspension loads are calculated for each layer. These values are summed and the fraction allocated to each layer is determined as a proportion of $\sum_{i=1}^{J} n_{z(i)}/n_{z(1)}$ where i represents a specified layer. The speed of suspended particles is assumed to equal that of the wind at each height (Mellor 1965).

The remaining transported load, $q - q_{sus}$, moves as saltation and creep. Little is known about creep load in either the eolian snow or sand environments. Ratios of creep to saltation transport of sand range from 0.065 to 0.249 and probably depend on grain size (Chepil 1945, Ishihara and Iwagaki 1950). The model considers creep load to be a constant fraction, 0.1, of the saltation load. This coefficient is weighted by a grain-size factor so that small grain size reduces creep transport. Particles in creep transport move primarily from the impact of saltating particles. Once this impetus is removed, as is the case beyond the flow separation point, particles in creep will have zero velocity. The speed of all particles in creep transport is therefore assumed to equal zero at the entrance to the mixing zone.

Two aspects of the final component of the total transport, the saltation load, are of particular importance. The average height of the saltation trajectories defines the lowest layer of suspension transport, at $z_{(1)}$, and the mean path length of saltating particles significantly affects the rate of drift infill near the flow separation point.

Most saltation of snow particles occurs close to the snow surface. From 70 to 80 percent of all transport occurs within 4 cm of the snow surface (Rusin 1959). Experiments by Kungurtsev (1956) showed that 73 to 91 percent of drifting snow was between 0 and 10 cm above the surface. The model calculates the mean height of saltating grains as either $U_*^2/2g$ (Owen 1964) or $\rho_f U_*^2/\rho_s g$ (Iversen et al 1976), where g is the acceleration of gravity, and ρ_f and ρ_s are air and snow particle densities.

Two options are used to calculate mean path length. For a depositional regime, Kobayashi (1972) provided a simple relationship between windspeed at 1 m height and path length, $L = 0.011\,U_1$, with L in meters and U_1 in m s^{-1}. Alternatively, a more complicated procedure incorporating estimates of the vertical velocity of saltating particles gives L equal to

$$(U_*^{1.5}\,U_z)-[2.5\,\ln(2gz/U_*^{2})]\,U_*^{2.5} \tag{7}$$

(Berg 1977). The total saltation transport is apportioned equally throughout several layers within the saltation transport zone.

Depositional Locations

The tractive force of the wind controls the snow particle deposition rate. Below a certain threshold windspeed, U_t, snow particles will not be transported. The drift surface is specified by the locus of points within the mixing zone or at the border of the mixing and eddy zones if U_t equals zero. These points represent the spatial location at which windspeed equals U_t. If U_t is assigned a value greater than zero, the potential drift surface will extend past the flow reattachment point and into the zone of boundary layer redevelopment. Exact specification of U_t is difficult since its value depends on secondary factors like grain shape and angularity (Williams 1964). Furthermore, most of the empirical information available involves observation of the windspeed at which movement is initiated rather than at which deposition starts. Factors such as surface hardness (Schmidt 1986) complicate the determination of U_t. The model uses U_t to differentiate areas of deposition and erosion, and based on available data (Berg 1977) uses 3 m s^{-1} as its value (at 1 m height).

The model defines a set of "accounting" cells, into which are parcelled the depositing snow particles. Taken together, the set of cells comprise the spatial configuration of the snowdrift. Each cell is rectangular and has a width of either 0.5 m or one that is user-defined. The cells are bounded at the base by the ground topography and at the top by the points in space where the windspeed equals U_t.

Windspeed and precipitation data allow calculation of blowing snow mass transport upwind of the drift catchment. Alternatively, blowing snow mass transport may be empirically observed. Windspeed and snow particle mass gradients with height above the ground or snow surface are determined, and at significant breaks in topographic slope the routines for airflow in the mixing and eddy zones and for particle trajectory are triggered. As the snow particles move through the mixing zone, each parcel of grains eventually crosses the separation streamline, alights in the redeveloping boundary layer zone, or passes beyond the catchment as "blowpast". The amount of blowpast is accounted for, and these particles may be deposited downwind in another drift. Up to three grain size fractions can be input to the model thus allowing investigation of layer relationships and stratification within the drift.

FIELD PROCEDURES

Field studies were conducted to analyze the drift accumulation model and to provide auxiliary information on other aspects of drift development. Input parameters to the model are primarily meteorological and topographic. Relevant environmental variables, specifically windspeed and direction, and blowing snow particle size and frequency, were measured. Topography was surveyed at two sites during the summers of 1973 and 1974, and drift accumulation at these sites was recorded during the winters of 1973-1974 and 1974-1975.

Study Site

Niwot Ridge is the most prominent alpine interfluve in the Indian Peaks region of the Colorado Front Range. It is an east-west trending spur on the east slope of the range, 35 km northwest of Boulder, (40°3'20" N, 105°35' W). Elevations range from 3450 to 3800 m, with several knobs upstanding along the central axis of the Ridge (fig. 2). Mean monthly windspeeds are high and were greater than 10 m s^{-1} between November and February, from 1952 to 1970. The snow accumulation period extends from mid or late October to mid May. Mean monthly air temperature maxima are below freezing from November to April. Winter precipitation is all snow and averages 100 mm per month (Barry 1973).

On Niwot Ridge, local relief results from the development of periglacial terraces and lobes on south and east-facing slopes. Benedict (1970:171) described "turf-banked terraces" as "bench-like accumulations of moving soil that lack conspicuous sorting." These landforms range up to 4 m in height at the riser, over 500 m long, and over 90 m wide, and often form a stair-step configuration (Benedict 1970). Depending upon aspect and windward tread orientation, snowdrifts form immediately leeward of the terrace lobes (fig. 3).

Drift accumulation was monitored at two terraces. The "Slope" Site on the leeward slope of a major topographic high point on Niwot Ridge includes five in-line snow accumulation troughs. The "Tank Trap" is a single trough usually retaining snow until mid August. The wind blows downslope into both sites (fig. 2).

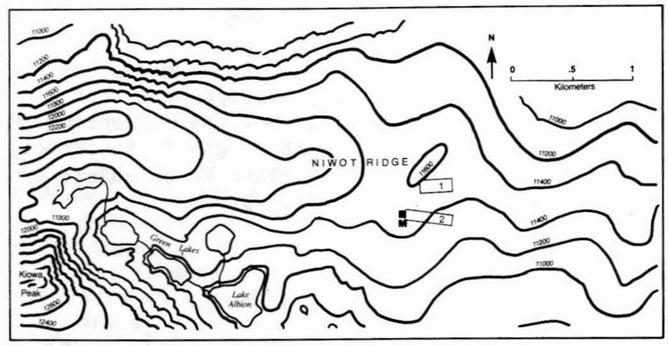

Figure 2.--Study site on Niwot Ridge, Colorado Front Range (Ward quadrange, USGS 7.5 Minutes Series). M represents location of the meteorological instruments. Drift accumulation sites are designated 1 (Slope Site) and 2 (Tank Trap). Elevations in feet.

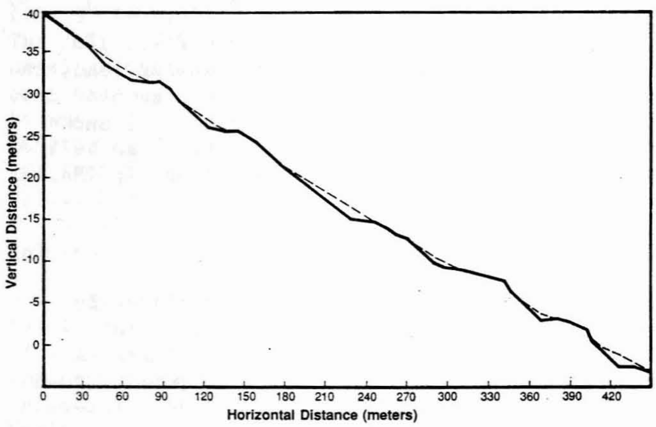

Figure 3.--Cross-sectional plot of ground (solid line) and snow (dashed lines) surfaces on Niwot Ridge, mid July 1974.

Drift Documentation

Terrain surveys during the summer provided ground control for the winter snow accumulation monitoring. Due to the high unidirectionality of snow-bearing winds on Niwot Ridge (Berg 1986), five profile lines (three at the Slope Site and two at the Tank Trap) constructed parallel to the dominant wind direction provided the main reference for winter monitoring. To compensate for possible errors in estimating the prevailing wind direction, additional lines were surveyed at 10° offsets to the main lines, providing topographic control over a 20° directional range. Use of the model at sites with highly variable wind directions is not recommended.

During winter, the spatial extent, depth, and timing of drift accumulation were surveyed. Accumulation stakes, 1.8 m in length, marked at 10-cm intervals, and positioned 3 m apart, allowed direct observation of snow depths during the initial accumulation period. Burial of the stakes forced a shift to abney level survey or probe measurements of snow depths. The time interval between drift surveys varied from 2 to 12 days and averaged 4 days. Before January 1 intersurvey intervals were shorter to assure identification of early season "slab" or near-cornice infill patterns.

Meteorological Observations

Primary meteorological variables input to the model were concerned with definition of the wind regime during each blowing snow event, the duration and magnitude of each event, and parameters of the blowing snow.

A three-cup anemometer and vane system (USDA 1970), positioned 8.75 m above ground level at a knoll approximately 200 m equidistant from the Slope Site and the Tank Trap, characterized airflow patterns (fig. 2). Hourly mean windspeed and wind direction were computed from the digitization of strip chart records.

Blowing snow was identified as particles passing through the sampling volume of a photoelectric device (Schmidt et al. 1984), moving in horizontal or near-horizontal trajectories, and having been either redistributed by the wind or entrained during precipitation. The "snow particle counter", which records particle size and frequency on a strip chart, was positioned 0.85 m above the ground. At that height particle sizes were expected to range from 0.1 to 0.2 mm and frequencies from 200 to 5000 particles per second--the calibration ranges of the instrument. Manual reduction of the strip chart data produced hourly minimum, median, and maximum particle size and frequency values. Wind and blowing snow were monitored between 2 November 1973 and 30 April 1974, and between 11 November 1974 and 7 May 1975 (Berg 1986).

TESTING THE MODEL

Two approaches were taken to analyze the model. First, its response to variations in selected input parameters was estimated to identify which relationships most affected the modelled outcome. Second, model "predictions" were compared with compatible empirical measurements of drift accumulation from the field observations.

Sensitivity Analysis

Values for 15 input parameters and constants were systematically varied, and changes in drift configuration and infill rate were compared with a standard six-event simulation. Details of the analysis are discussed elsewhere (Berg 1977); only the significant results are reported here.

Changes in most of the input parameters had a regular and predictable influence on the model outcome, e.g., larger grain size and less angularity increased particle fall velocity and particle deposition near the top of the trough. Similarly, greater free-stream velocity shifted more of the transport into the suspension mode at the expense of the saltation load, shifted the bulk of the suspension load to higher atmospheric levels, and increased windspeed at all levels above the surface. These factors combined to increase the amount of snow blowing past the trough and to spread deposition more evenly within it. In general, however, the proportion of total transport blowing past the trough remained constant and relatively low, at about 10 percent of total transport, until the trough was about 80 percent filled, after which blowpast increased sharply.

As expected, the windspeed parameters strongly influenced the timing and degree of drift infill. At windspeeds under 20 m s^{-1}, all particles moving in saltation settled immediately to the lee of the flow separation point. Deposition downwind was maximized at moderate windspeeds. At higher windspeeds blowpast predominated, while at lower speeds energy was insufficient to propel particles far leeward.

Three other parameters, the lower mixing region angle β, the windward terrain approach angle, and the threshold speed for particle entrainment/ deposition, acted alone or together to profoundly influence drift shape by specifying the accumulation surface and the flow reattachment point. Airflow with a downward approach to the trough foreshortened the drift by shortening the suspension particle trajectories (fig. 4). Conversely, an upward terrain approach lengthened the suspension particle trajectories (fig. 5) and consequently, dominance of creep and saltation deposition increased cornice-like formations, often in association with increased blowpast of particles in suspension.

The β and U_t parameters determine the heights of the accounting cells and thereby the spatial location of the drift surface. As U_t increased, the cell height within the mixing zone rose, thereby raising the surface of the potential drift. At the extreme, if U_t is greater than approximately one-half of the upwind flow velocity, the potential drift surface could rise and conceivably not intersect the ground surface surface downwind. Given realistic U_t and upwind flow velocities, however, this eventuality is extremely unlikely. As β increased, the dip of the potential drift surface steepened as the separation bubble shortened. In this condition, much of the suspension transport blows past the trough.

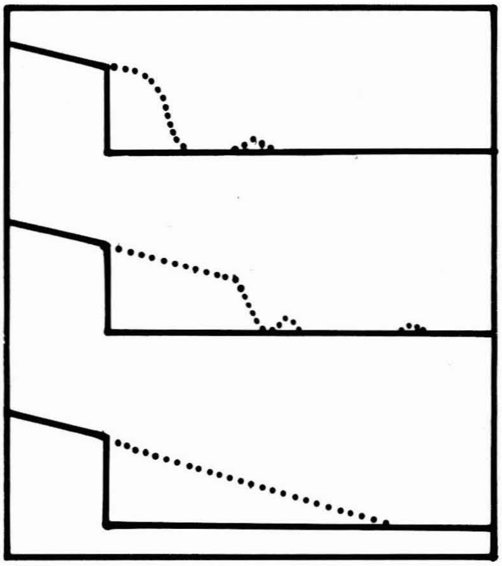

Figure 4.--Sensitivity analysis with downslope terrain approach (slope angle = 15°). Three sequential blowing snow events are simulated.

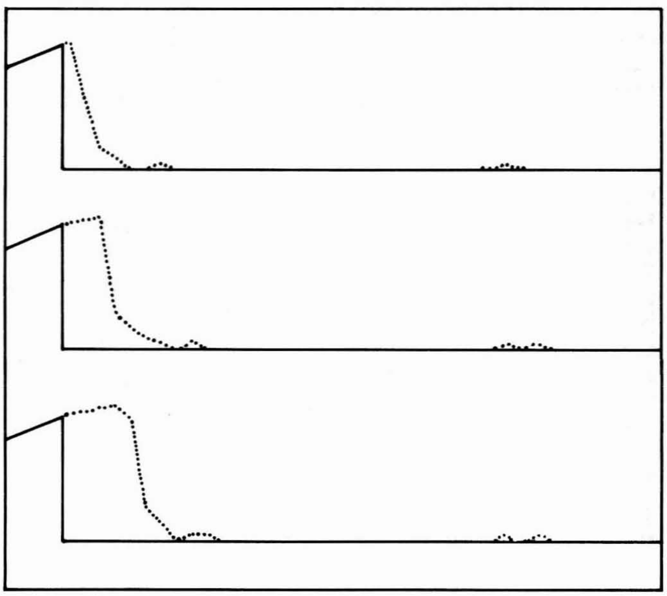

Figure 5.--Sensitivity analysis with upslope terrain approach (slope angle = -10°). Three sequential blowing snow events are simulated. Input values for all quantities other than approach slope angle are identical to those in figure 4.

Comparison with Field Observations

Field observations from two of the lines established on the sites, the south line at the Tank Trap and the north line at the Slope Site, were chosen for comparison with the modelled output. Only the first month's accumulation during 1974 was considered because it was adequate to illustrate most of the comparative features. Drifts were monitored on October 15, 16, 20, 24, and 28, and on November 1, 5, and 11. The point of initial accumulation was chosen as a major break in slope (fig. 6). Boundary layer thickness was assumed to equal 10 m, and the windspeed at this height was calculated as a logarithmic law extrapolation from the windspeed measured at 8.75 m height. A 12-hour time frame was used to sequence the model.

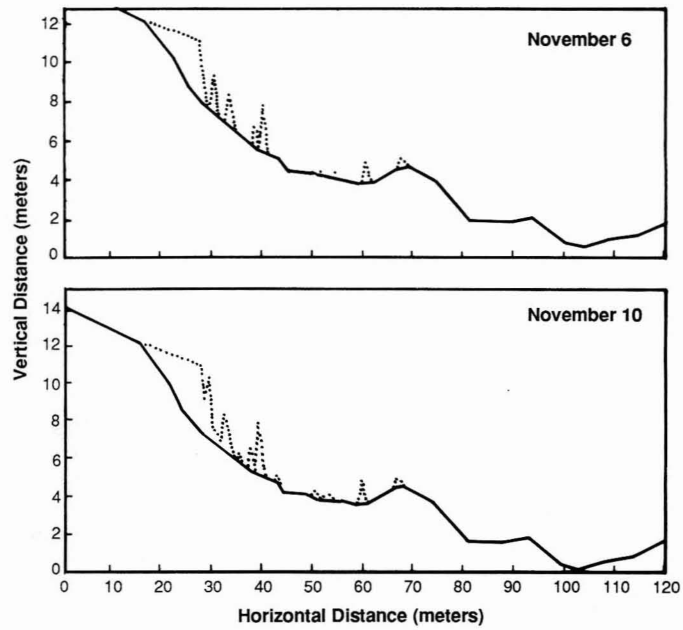

Figure 6.--Modelled snowdrift development along Slope Site, North line. Vertical exaggeration is 3.7 fold.

Close inspection of figures 6 and 7 shows discrepancies in deposition beyond the drift cornice: jagged peaks of accumulation, insufficient deposition at the flow separation point and downwind of it on the modelled profile during the latter stages of the test period, and a lack of accumulation for the modelled output in the second trough (at 75 to 90 m).

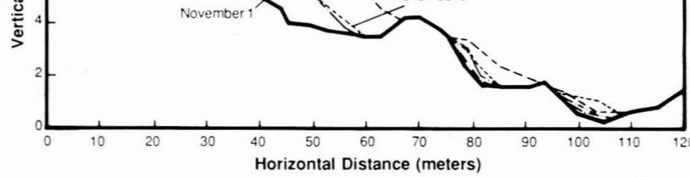

Figure 7.--Observed North Slope Site drift infill. Vertical exageration is fivefold.

The ragged profile of the modelled deposition pattern is due partially to the fact that the model segregates the lower atmospheric layer into discrete layers rather than treating it realistically as a continuum (fig. 6). Refinement of the model to depict the snow surface as a running mean of snow depths in adjacent cells would even out the surface.

Comparison between matched or interpolated cross-sectional areas measured in the field with those calculated by the model showed approximately a 60 percent underestimate by the model (table 1). This underestimate may result from underestimated total mass transport, excessive blowpast, or low density of drifted snow. The method for determining transport uses the intermediate value calculated from six possible empirical formulas. It would be possible to use a different relationship so as to increase total transport although there is no clear justification for doing so. Alternatively, use of more grain size fractions with most of the transport allocated to the larger sizes should reduce blowpast and consequently increase total cross-sectional area. More fractions, however, might also reduce deposition downwind from the flow separation point. Perhaps the easiest modification would be to increase drift density from 0.25 to 0.5 g cm^{-3}, as suggested by Santeford (1972), to increase accumulation at all cell locations substantially.

Table 1.--Cross-sectional areas (m^2) of snowdrifts, Niwot Ridge, 1974.

Site	Date	Observed	Modelled
South Line, Tank Trap	10/15	16.9[1] 13.0[2]	12.9[3]
	10/16	8.1	13.8
	10/31	----	26.2
	11/1	45.3	----
	11/4	----	26.8
	11/5	40.2	----
North Line, Slope Site	10/15	24.9	10.9
	10/16	23.3	11.8
	10/31	----	24.9
	11/1	68.2	----
	11/4	----	26.5
	11/5	71.6	----
	11/6	----	29.0
	11/10	----	35.4
	11/11	107.2	----

[1]0900 hours. [2]1500 hours. [3]All modelled values are at 1200 hours.

The model did not adequately simulate drift accumulation in nearby downwind troughs. The model treated the entire horizontal space between 17 and 110 m as one mixing/eddy zone, which is improper given the topography shown in figures 6 and 7. Secondary separations probably occurred at 75 and 94 m. The model should be refined to accommodate multiple in-line troughs.

SUMMARY

A computer simulation model was developed for estimation of the location and extent of natural snowdrift accumulation on heterogeneous terrain. Observations on experimentation with the model show that:

- snow particle deposition is greater immediately beyond the flow separation point than further downwind from it;
- smaller diameter particles carry farther and are deposited further downwind;
- windspeed is a major determinant in the amount and location of snow deposition in that a) as speed increases particles go into suspension transport--at the expense of saltation and creep transport--and are more likely to blow past the trapping site, b) an increase in speed lengthens the horizontal component of the particle trajectory to similarly promote blowpast, and c) deposition downwind from the flow separation point is maximized at moderate windspeeds; at higher speeds blowpast predominates while at lower speeds there is insufficient energy to propel particles far leeward;
- at windspeeds under 20 m s^{-1}, all particles moving in saltation settle immediately to the lee of the flow separation point;
- ground topography windward of the trap is influential in determining the amount of infill. A downslope upwind approach slope shortens the drift accumulation relative to a horizontal approach slope. A moderate upslope approach lengthens the drift, increases infill due to a reduction in blowpast, and promotes cornice development;
- the proportion of the total transport blowing past the trap remains constant and low, approximating 10 percent of total transport, until approximately 80 percent of the trap is
- the model extends the cornice infill stage of drift development for a much longer time period than observed in the field.
- drift cross-sectional areas are underestimated approximately 60 percent by the model. Raising the snow density input value would rectify much of the underestimate.
- improvements are needed to adequately predict drift accumulation for two or more nearby inline catchments.

ACKNOWLEDGEMENTS

This study was supported by the Institute of Arctic and Alpine Research, University of Colorado, and the Rocky Mountain Forest and Range Experiment Station, Forest Service, U.S. Department of Agriculture. Field assistance was furnished by Elizabeth Berg and Frederick Bauer. Without the patient encouragement of Nel Caine and R.A. Schmidt this study would not have been completed. Carl Benson, Nel Caine, Bruce McGurk, and Richard Minnich made valuable comments on an earlier draft of this manuscript.

LITERATURE CITED

Abramovich, G.K. 1963. The Theory of Turbulent Jets. MIT Press, Cambridge, Mass. 347 p.

Allen, J.R.L. 1968. Current Ripples. North-Holland Pub. Comp., Amsterdam. 433 p.

Barry, R.G. 1973. A climatological transect on the east slope of the Front Range, Colorado. Arctic and Alpine Research 5:89-110.

Benedict, J.B. 1970. Downslope soil movement in a Colorado alpine region: rates, processes, and climatic significance. Arctic and Alpine Research 2:165-226.

Berg, N.H. 1977. Prediction of natural snowdrift accumulation on alpine ridge sites. Ph.D. dissertation, Univ. Colorado. 310 p.

Berg, N.H. 1986. Blowing snow at a Colorado alpine site: measurements and implications. Arctic and Alpine Research 18(2):147-161.

Budd, J. 1966. The drifting of non-uniform snow particles. In: M. Rubin (ed.), Studies in Antarctic Meteorology. Antarctic Research Series, vol. 9, Amer. Geophys. Union. p. 59-70.

Budd, W., Dingle, R., and U. Radok. 1966. The Byrd snow drift project: outline and basic results. In: M. Rubin (ed.), Studies in Antarctic Meteorology. Antarctic Research Series, vol. 9, Amer. Geophys. Union. p. 71-134.

Chepil, W.S. 1945. Dynamics of wind erosion: II. Initiation of soil movement. Soil Sci. 60:397-411.

Ishihara, T. and Y. Iwagaki. 1950. Studies on the countermeasures to prevent Alior Harbor from filling up with sand drift. Bulletin of the Committee for the Countermeasure of Sand Drift, Tottori Prefecture. (In Japanese). Cited in Horikawa, K. and H.W. Shen. 1960. Sand movement by wind. U.S. Army Corps of Engineers, Beach Erosion Board. Tech. Memo. 119. 51 p.

Iversen, J.D., Pollack, J.B., Greeley, R. and B.R. White. 1976. Saltation threshold on Mars: the effect of interparticle force, surface roughness, and low atmospheric density. Icarus 29:381-393.

Jopling, A.V. 1960. An experimental study on the mechanics of bedding. Ph.D. dissertation, Harvard Univ. 358 p.

Kobayashi, D. 1972. Studies of snow transport in low-level drifting snow. Inst. Low Temp. Sci., Ser. A, Contrib. 24. 58 p.

Kungurtsev, A.A. 1956. The transfer and deposition of snow. Cold Reg. Res. and Engin. Lab., Tech. Rept. 258. 27 p.

Martinelli, M. Jr. 1975. Watershed yield improvement from alpine areas: the status of our knowledge. Forest Serv., U.S.D.A., Res. Pap. RM-138. 16 p.

Mellor, M. 1965. Blowing snow. Cold Reg. Sci. and Eng. Lab., Mono., Pt. 3, Sec. A3c. 79 p.

Mellor, M. and U. Radok. 1960. Some properties of drifting snow. Proc., Symposium on Antarctic Meteorology. Melbourne, Pergamon Press. London. p. 333-346.

Minnich, R.A. 1984. Snow drifting and timberline dynamics on Mt. San Gorgonio, California, U.S.A. Arctic and Alpine Research 16(4):395-412.

Naib, S.K.A. 1966. Mixing of subcritical stream in a rectangular channel expansion. J. Inst. Water Engrs. 20:199-206.

Outcalt, S.I. and D.D. MacPhail. 1965. A survey of neoglaciation in the Front Range of Colorado. University of Colorado, Series in Earth Sciences, 4. 124 p.

Owen, P.R. 1964. Saltation of uniform grains in air. J. Fluid Mech. 20:225-242.

Perla, R.I. and M. Martinelli. 1976. Avalanche Handbook. U.S.D.A. Agriculture Handbook 489. 289 p.

Radok, U. 1968. Deposition and erosion of snow by the wind. Cold Reg. Res. and Eng. Lab., Res. Rept. 230. 23 p.

Rusin, N.P. 1959. Horizontal transport of snow in Antarctica. Cold Reg. Res. and Eng. Lab., Translation. 1970. 31 p.

Santeford, H.S. 1972. Management of windblown alpine snow. Colorado State Univ., Atmos. Sci. Pap. 192.

Schmidt, R.A. 1972. Sublimation of wind-transported snow--a model. Forest Serv., U.S.D.A., Res. Pap. RM-90. 24 p.

Schmidt, R.A. 1986. Snow surface strength and the efficiency of relocation of snow. Proc., Cold Regions Hydrology Symposium. Amer. Water. Resour. Assoc. Bethesda, Maryland. p. 355-358.

Schmidt, R.A., Meister, R., and H. Gubler. 1984. Comparison of snow drifting measurements at an alpine ridge crest. Cold Reg. Sci. and Tech. 9:131-141.

U.S. Department of Agriculture, Forest Service. 1970. Instrumentation for snow, weather, and avalanche observations; Snow Safety Guide 2. Alta Avalanche Study Center. 80 p.

Williams, G. 1964. Some aspects of the eolian saltation load. Sedimentology 3:257-287.